frontiers | Frontiers in Materials

TYPE Original Research
PUBLISHED 27 February 2023
DOI 10.3389/fmats.2023.1125869

OPEN ACCESS

EDITED BY
Muhammad Sufyan Javed,
Lanzhou University, China

REVIEWED BY
Imtiaz Khan,
The University of Manchester,
United Kingdom
Muhammad Yaqub,
Kumoh National Institute of Technology,
Republic of Korea

*CORRESPONDENCE
Shahid Iqbal,
shahidgcs10@yahoo.com
Humayun Ajaz,
humayunajaz@uet.edu.pk
Ali Bahadur,
abahadur@wku.edu.cn

SPECIALTY SECTION
This article was submitted to Polymeric and Composite Materials,
a section of the journal Frontiers in Materials

RECEIVED 16 December 2022
ACCEPTED 18 January 2023
PUBLISHED 27 February 2023

CITATION
Umar M, Mansoor S, Javed M, Hussain N, Bajaber MA, Iqbal S, Alhujaily A, Mohyuddin A, Ajaz H, Rauf A, Bahadur A, Al-Fawzan FF and Elkaeed EB (2023), Fabrication of novel oxochalcogens halides of manganese and tin nanocomposites as highly efficient photocatalysts for dye degradation and excellent antimicrobial activity.
Front. Mater. 10:1125869.
doi: 10.3389/fmats.2023.1125869

Fabrication of novel oxochalcogens halides of manganese and tin nanocomposites as highly efficient photocatalysts for dye degradation and excellent antimicrobial activity

Misbah Umar[1], Sana Mansoor[2], Mohsin Javed[2], Nadia Hussain[3,4], Majed A. Bajaber[5], Shahid Iqbal[6]*, Ahmad Alhujaily[7], Ayesha Mohyuddin[2], Humayun Ajaz[1]*, Abdul Rauf[1], Ali Bahadur[8]*, Foziah F. Al-Fawzan[9] and Eslam B. Elkaeed[10]

[1]Department of Chemistry, University of Engineering and Technology Lahore, Lahore, Pakistan, [2]Department of Chemistry, School of Science, University of Management and Technology, Lahore, Pakistan, [3]Department of Pharmaceutical Sciences, College of Pharmacy, Al Ain University, Al Ain, Abu Dhabi, [4]AAU Health and Biomedical Research center, Al Ain University, UAE, Abu Dhabi, [5]Chemistry Department, Faculty of Science, King Khalid University, Abha, Saudi Arabia, [6]Department of Chemistry, School of Natural Sciences (SNS), National University of Science and Technology (NUST) H-12, Islamabad, Pakistan, [7]Biology Department, College of Science, Taibah University, Al Madinah Al Munawarah, Saudi Arabia, [8]Department of Chemistry, College of Science and Technology, Wenzhou-Kean University, Wenzhou, China, [9]Department of Chemistry, College of Science, Princess Nourah bint Abdulrahman University, Riyadh, Saudi Arabia, [10]Department of Pharmaceutical Sciences, College of Pharmacy, AlMaarefa University, Riyadh, Saudi Arabia

The dark brown and white crystals of manganese and tin ($Mn_2Se_3Cl_2O_7$ and $SnSe_3O_4Cl$) have been synthesized by solid-state reaction at 450 C. The morphology and the elemental analysis of newly synthesized compounds were studied by SEM and EDX Analysis. SEM analysis reveals that the particle size for $Mn_2Se_3Cl_2O_7$ was found to be 0.2–2.5 μm and for $SnSe_3O_4Cl$ 2.0–6.0 μm. The EDX studies showed the presence of Mn, Se, O, Cl, and Sn elements. Powdered XRD confirmed the presence of a new phase present in these compounds. Under UV-vis irradiation, the kinetics of methylene blue (MB) degradation catalyzed by produced nanoparticles were monitored. The dye degradation efficiency was estimated, and results reveals that after 150 min of irradiation, almost 75% of the dye was degraded in the presence of Mn compound while 71% degradation was shown by Sn compound. Both composites display antimicrobial activity against *Staphylococcus aureus* and *Escherichia coli* with a maximum value of 34.5 mm. The maximum antimicrobial activity shown by Mn-incorporated nanocomposites estimated at 32.5 mm was against Gram-positive bacteria and 26.4 mm against Gram-negative bacteria. Similarly, the maximum antifungal activity shown by Sn incorporated estimated at 33.9 mm was compared to Gram-positive bacteria and 27.8 mm against Gram-negative bacteria.

KEYWORDS

solid state, degradation, heterojunction, methylene blue, antimicrobial activity

Introduction

Industrial wastes, especially waste liquids of synthetic dyes used in the paper, food, agriculture, leather, textile and pharmaceutical industries (Farahmandjou and Abaeiyan, 2017; Altaf et al., 2020a) are highly toxic and biodegradable organic wastes that are critical to the survival of organisms, becoming the biggest problem (Sivagowri and Shivatharsiny, 2018). .Water is the most important element for life on Earth. Due to rapid population growth, the demand for water is increasing day by day (Shanmugaratnam, Rasalingam; Lv et al., 2020). Many scientists have focused and worked on efficient techniques for removing these non-biodegradable industrial pollutants from wastewater before they enter the environment (Peng et al., 2020). Several techniques such as adsorption, chlorination, filtration, and air stripping, coagulation, and membrane processes are traditional methods of treating water that are costly, time-consuming, and sometimes hazardous (Ranson et al., 2015; von Gunten, 2018; Bethi et al., 2016).

The treatment of drinking water has given rise to the advanced oxidation process (AOPs). Numerous AOPs are accessible, including moist air oxidation, electrochemical oxidation, hydrogen peroxide, heterogeneous photocatalysts, and supercritical water oxidation (Chen et al., 2018). The semiconductors with lower bandgaps that can produce electrons to interact with water molecules are in a distinct phase from the reaction system in heterogeneous photocatalytic AOPs. The semiconductors utilized as a catalyst for AOPs need to be affordable, easily accessible, stable, and chemically inert. They also need to demonstrate strong photocatalytic activity and low toxicity. In order to degrade organic molecules by photocatalysis, a variety of materials and agents are accessible, including simple metal oxides, transition metal oxides, nitrides, and complex oxides (O'Shea and Dionysiou, 2012).

A catalytic reaction in which light is absorbed by a substrate is referred to as photocatalysis by the International Union of Pure and Applied Chemistry (IUPAC) (Schneider et al., 2016). When a semiconductor photocatalyst is exposed to light with photon energies above the bandgap energy, electrons in the valence band (VB) are stimulated to the conduction band (CB), leaving holes in VB. Due to the fact that photocatalytic reactions take place on the surface of the photocatalyst, the photoinduced free charge carriers must first diffuse to the active sites on the photocatalytic surface in order to cause the reaction (Mills and Le Hunte, 1997; Castellote et al., 2011; Photocatalysis, 2016). The distance between the substrate's redox potential and the semiconductor photocatalyst's band edge, however, determines whether a chemical reaction can take place on the semiconductor photocatalyst on that substrate (Thermodynamic, 2012; Liu et al., 2014; Ohtani, 2014).

Researchers have been captivated by selenide compounds of different transition metal oxides due to their significant potential for use in industrial applications such as semiconductors, IR detection, energy storage devices, laser diodes, catalysis, photovoltaic electronics, and photo-detective devices. The creation of inorganic semiconductor nanocomposites has caught the interest of scientists because of their novel characteristics, including reactivity, low melting point, electrical properties, optical properties, and magnetic properties. Compared to their bulk counterparts, nanomaterials have a high surface area-to-volume ratio (Ou et al., 2017). Under solar radiation, a process known as photocatalytic breakdown, the high reactivity of nanocomposites is crucial for the removal of organic contaminants from polluted water (Jabeen et al., 2017; Ye et al., 2018). For inorganic semiconducting nanocomposites, bandgap engineering and particle size control are considered essential tools to tailor their properties for different applications across multiple industries (Zhang et al., 2004). Nanocomposites have gained a lot of attention from researchers due to their wide range of applications. Nanocomposites are those materials that contain nanoscale particles within a matrix of conventional materials. The applications of nanocomposites are in the field of biomedicine, storage devices, food and environmental sciences, electronic industry, and automotive fields. The characteristic properties of nanocomposite materials are that they are easy to synthesize, exhibit high mechanical properties, and are thermally very stable.

The chemistry of selenites (SeIV) and selenates (SeVI) has undergone extensive development during the past 20 years (Choudhury et al., 2002; Krivovichev et al., 2005; Song et al., 2014; Zhao et al., 2014; Kovrugin et al., 2015a; Berdonosov et al., 2018). Due to the interaction of selenite groups, metals, and halide ions in soft-soft and hard-hard interactions, metal oxyhalides with selenite anions exhibit a complex and varied crystal chemistry (Aliev et al., 2014; Kovrugin et al., 2015b; Kovrugin et al., 2015c; Kovrugin et al., 2016; Charkin et al., 2017; Kovrugin et al., 2017).

The transition metals can bond with both halides and oxides ions in the transition metals oxo halides. The lone pair on the chloride ion and stereo chemically active Se^{+4} both performed the function of "Chemical Scissors" resulting in the formation of low dimensional arrangement (Johnsson et al., 2003; Zhang et al., 2009) and open crystal structures which shows magnetic frustration such as $Cu_2Te_2O_5X_2$ and $FeTe_2O_5X$ (X = Cl, Br) (Johnsson et al., 2000; Becker et al., 2006). Up till now many transition metal oxo-chalcogen halides are formed $Co_5(SeO_3)_4Cl_2$ (Becker et al., 2007a), $Cu_5(SeO_3)_2O_2Cl_2$ (Galy, 1979), $Ni_5(SeO_3)_4Cl_2$ (Shen et al., 2005), β-$Cu_3(SeO_3)_2Cl_2$ (Becker et al., 2007b), $Cu_5(SeO_3)$ OCl_5 (Krivovichev et al., 2004), $Cu_5(SeO_3)_2O_2Cl_2$ (Millet et al., 2001), $Cu_9(SeO_3)_4O_2Cl_6$ (Bastide et al., 2000), $Cu_3(SeO_3)_2Cl_2$ (Millet et al., 2000), β-$Cu_9(SeO_3)_4O2Cl_6$ (Zhang et al., 2010), α-$Cu_3(SeO_3)_2Cl_2$ (Semenova et al., 1992), $Zn_2(SeO_3)$ Cl_2 (Ijaz, 2007), $InTeO_3Cl$ (Alonso, 1998), $SbTeO_3Cl$ (Secuk et al., 2014), $Co_2SeO_3(OH)_2$ (Zhong and DanruiNi, 2020).

In the present work, a simple, cost-effective solid-state method was used to synthesize the metal selenium Oxo-halides of Mn and Sn. The characterization technique like XRD and SEM-EDX were used to analyze the new phase, structure, and composition of the compound. Moreover, the optical and antimicrobial activity was also studied. The main purpose of this study was to form the novel transition metal selenium Oxo-halides with more effective optical and antibacterial activity.

Experimental section

Chemicals

$MnCl_2.H_2O$ and SeO_2 and $SnCl_2$ and Se used as starting material for the synthesis of $Mn_2Se_3Cl_2O_7$ and $SnSe_3O_4Cl$ were purchased directly from Sigma Aldrich with 99% purity and used directly without further purification. Double distilled water was used to obtain a high-purity product. The Methylene blue dye used was of analytical grade.

FIGURE 1
Schematic diagram of Solid State Synthesis.

Fabrication of $Mn_2Se_3Cl_2O_7$ and $SnSe_3O_4Cl$

For the synthesis of $Mn_2Se_3Cl_2O_7$, $MnCl_2.H_2O$ and SeO_2 were taken as a starting material in a stoichiometric ratio of 1:2 (0.323 g and 0.443 g). Whereas for the synthesis of $SnSe_3O_4Cl$, solid $SnCl_2$ was reacted with elemental selenium in the stoichiometric ratio of 1:8 (0.947 g and 3.115 g) respectively. After introducing the mixture into the crucibles, these were placed in a preheated muffle furnace at 450 C for 48 h (Rabbani et al., 2019). The dark brown crystal products were obtained after washing with distilled water followed by acetone. The resultant product obtained was dried in an oven at 80 ˚C Figure 1 for 2 hrs and saved for further characterization.

Photocatalytic activity

To study the photocatalytic activity of synthesized compounds, 0.2 g of the compound was taken in the beaker containing 100 mL of MB dye. The solution was stirred for 30 min to attain absorption equilibrium the mixture was irradiated in direct sunlight. 5 mL solution was taken out after regular intervals (30 min) and check the absorption at the UV- Vis Spectrophotometer. The proportion degradation of dye in the presence and absence of compounds was calculated by formula (Pouretedal et al., 2009)

$$\%D = Co - Ct/Co \times 100$$

Antimicrobial activity

The antimicrobial activity was examined by using the disc diffusion method against pathogenic bacterial strains (*Escherichia coli* and Staphylococcus *aureus*) (Altaf et al., 2020b). For 30 min, nutrient agar containing the following ingredients was placed in the autoclave: peptone 5, beef extract 1, yeast extract 2, sodium chloride 5, and agar 20. With the aid of sterile culture swabs, fresh cultures of each test organism containing 1 of the colony-forming units (CFU)/ml were applied to nutrient agar plates to grow bacteria. Different dilutions (0.25, 0.5, and 1 mg/mL) were then developed to test the susceptibility of the prepared nanocomposites. The negative control utilized was deionized water (DIW). After being soaked in l of these dilutions, discs were placed on agar plates and incubated for 24 h in an aerobic environment at 37 C. Zone of inhibition was evaluated on a meter scale (mm) at various values (Image J software). By doing the experiment three times, the repeatability and reliability of the results were verified.

Instrumentation

The microcrystalline phase information of Mn2Se3Cl2O7 and SnSe3O4Cl was investigated using PAAnlytical Xpert PRO X-ray diffraction (XRD) and Cu Kα radiation (λ ~ 1.5406 Å), yielding data in the 2θ range 5˚–80˚. Using a FE-SEM (JSM-6460LV) coupled to an EDX analyzer, the morphological properties and composition of the goods were ascertained. Using a Genesys 10S UV-visible spectrophotometer, optical absorption spectra in the 120–1,100 nm range were examined.

Results and discussion

Powder X-Ray diffraction analysis (XRD)

The resulting synthesized compound i.e., $Mn_2Se_3Cl_2O_7$ and $SnSe_3O_4Cl$ firstly ground and homogenized and placed on the sample holder of XRD (D8- Discoverer Bruker Germany) and measured 2°θ from 15–90˚ for almost 30 min. The search match procedure was done by using XPERT-HIGHSCORE. The result showed that the powder XRD pattern of both compounds did not match with the binary and tertiary compounds of metal oxo chalcogen halides of given elements i.e., Mn and Sn Figure 2 indicated that there must be some new phase present in the compound which makes it novel from other known compounds.

Scanning electron microscopy (SEM)

The result obtained from SEM as shown in Figure 3 showed that the newly formed compound $Mn_2Se_3Cl_2O_7$ exhibits well-defined

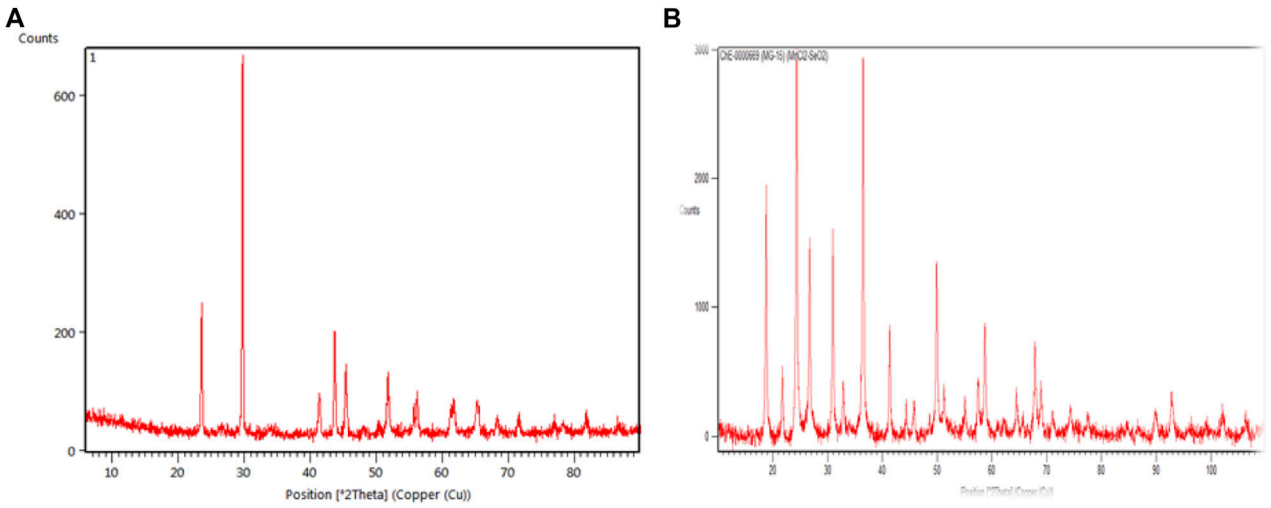

FIGURE 2
XRD pattern of synthesized compound **(A)** XRD of $Mn_2Se_3Cl_2O_7$ **(B)** XRD pattern of $SnSe_3O_4Cl$.

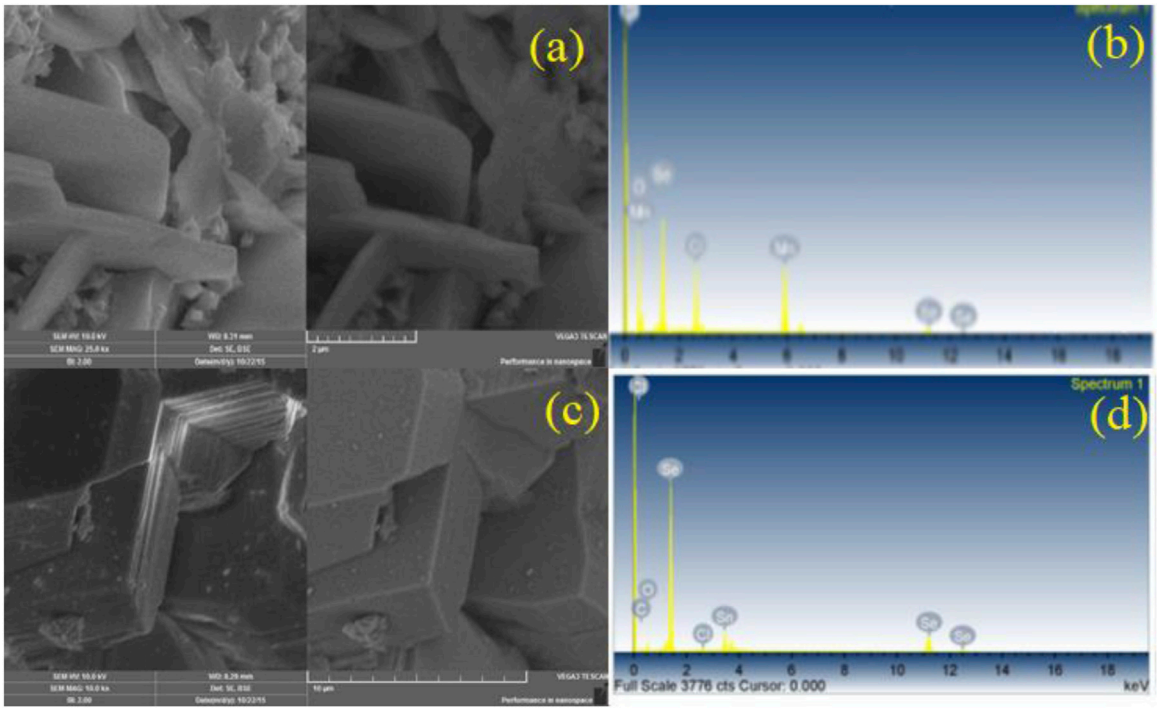

FIGURE 3
SEM-EDX of newly synthesized compounds **(A)** SEM image of $Mn_2Se_3Cl_2O_7$ **(B)** EDX of $Mn_2Se_3Cl_2O_7$ **(C)** SEM image of $SnSe_3O_4C$ **(D)** EDX of $SnSe_3O_4C$.

edges and a smooth surface with a rod-like arrangement having a particle size ranging from 0.2–2.5 µm. While the SEM graph of $SnSe_3O_4Cl$ shows that this compound has layers arrangement with particle size ranging from 2.0–6.0 µm.

The elemental analysis and their stoichiometry were carried out with the help of an EDX-Spectrometer (EDX, LINK AN10000). The spectrum of $Mn_2Se_3Cl_2O_7$ confirmed the atom's stoichiometry in the compound and provided the mean compositional analysis of the compound Table 1.Whereas the EDX spectrum of $SnSe_3O_4Cl$ insured the presence of all the elements (Sn, Se, O_2, Cl) in specific ratio.

For the photocatalytic activity of two synthesized compounds against methylene Blue (MB) dye, 100 mL of MB dye was taken in a Petri dish with the addition of 0.2 mg of samples. To achieve absorption-desorption equilibrium between the dye and produced

TABLE 1 Atomic percentage of the elements present in newly synthesized compounds through EDX.

$Mn_2Se_3Cl_2O_7$		$SnSe_3O_4Cl$	
Elements	Atomic %	Elements	Atomic %
Mn	14.28	Sn	14.035
Se	21.41	Se	34.95
O	50	O	41.35
Cl	14.28	Cl	9.65

chemicals, the reaction mixture was agitated for 30 min in the dark prior to exposure to radiation. These Petri dishes were placed in direct sunlight for irradiation. 5 mL of the sample was taken out at regular intervals (every 30 min) during light irradiation, filtered, and centrifuged to obtain a pure solution (Shanmugam et al., 2015). Then the filtrate is subjected to a UV-Visible spectrometer and photodegradation was calculated by using the equation as follows.

$$\%D = Co - Ct/Co \times 100 \quad (1)$$

Figure 4 shows the dye degradation during the different intervals of time under light irradiation in the presence of two synthesized compounds. As more hydroxyl radicals are generated as a result of increased radiation falling on the catalyst surface, the degradation efficiency rises. So with the passage of time, more and more free radicals of oxygen are formed which are responsible for the degradation of organic dye. The percentage degradation was calculated by Eq. 1 and values are shown in Table 2. The data clearly shows that after 150min of irradiation, almost 75% of the dye was degraded in the presence of Mn compound while 71% degradation was shown by Sn compound. The rate constant for the degradation of dye was calculated by a first-order reaction equation (Kannadasan et al., 2014).

$$\ln Co/Ct = kt \quad (2)$$

Where k is the rate constant. Figure 5 shows the plot illustrating the linear relationship between time and ln C_o/C_t and from the slope of the graph, the rate constant is calculated. The value of the rate constant for the $SnSe_3O_4Cl$ compound is 0.00378 min^{-1} whereas the rate constant value of the $Mn_2Se_3Cl_2O_7$ compound is 0.00447 min^{-1} which shows that increases in rate constant value increase the efficiency for photodegradation.

The Possible Mechanism for Photocatalytic Degradation

During light irradiation, some electrons from the valance band make a quantum jump to the conduction band and move to the

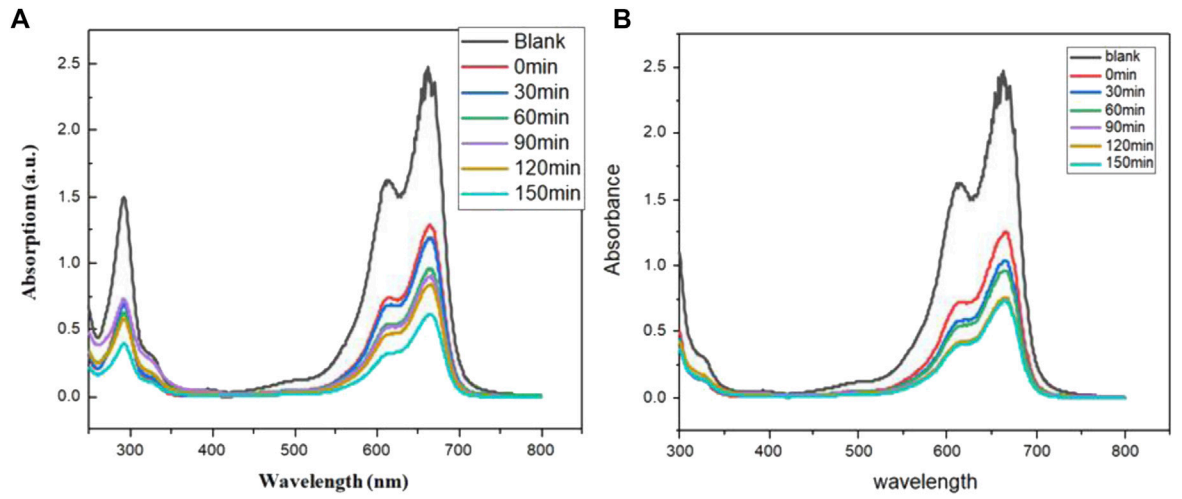

FIGURE 4
Dye Degradation of Methylene blue **(A)** Degradation of MB dye in Mn2Se3Cl2O7 **(B)** Degradation of MB dye in SnSe3O4Cl.

TABLE 2 Percentage degradation of $Mn_2Se_3Cl_2O_7$ and $SnSe_3O_4Cl$.

Time (Min)	*% Degradation of $Mn_2Se_3Cl_2O_7$*	*% degradation of $SnSe_3O_4Cl$*
0	48	48
30	52	58
60	61	60
90	63	68
120	66	69
150	75	71

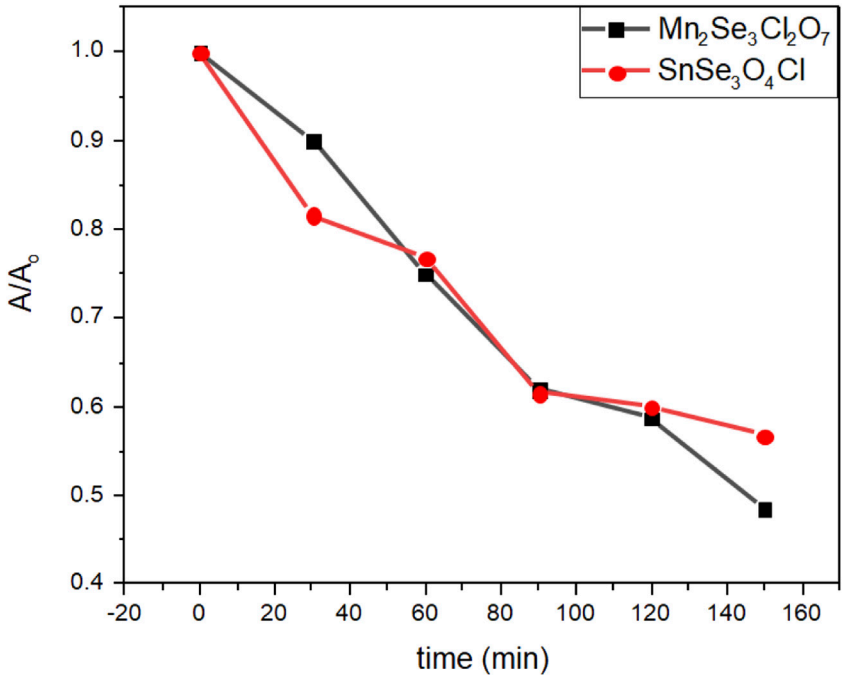

FIGURE 5
Degradation ratio Vs. time.

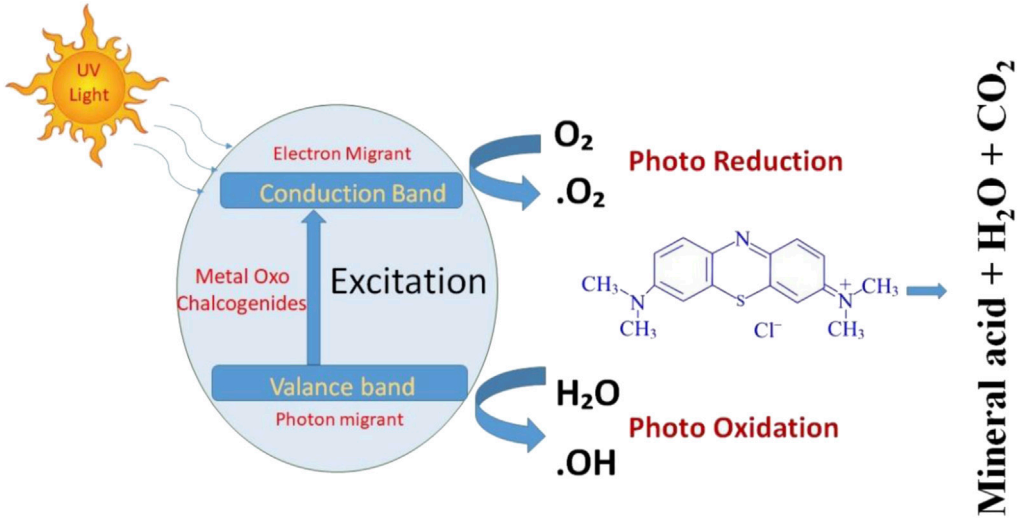

FIGURE 6
Mechanism for photocatalytic activity.

surface for surface reaction. These electrons from the surface react with the absorbed oxygen to form oxygen radicals. The concentration of oxygen is responsible for the efficiency of photo-degradation. And the holes in the valance band form during the excitation and react with water molecules to produce hydroxyl radicals. The two oxygen radicals and hydroxyl radicals are accountable for the oxidative photo-degradation of methylene blue. The Possible Mechanism for Photocatalytic Degradation is shown in Figure 6.

Antibacterial and antifungal activity

The disc diffusion method was used to analyze the bacterial sensitivity against the synthesized compounds as shown in Figure 7. The zone inhibition was measured against Gram-positive and Gram-negative bacteria ranging from 0 mm to 32.4 mm in diameter. The outcomes show an additive effect of nanocomposites' concentrations and inhibition zones (mm). For the nanocomposite

10.3389/fmats.2023.1125869

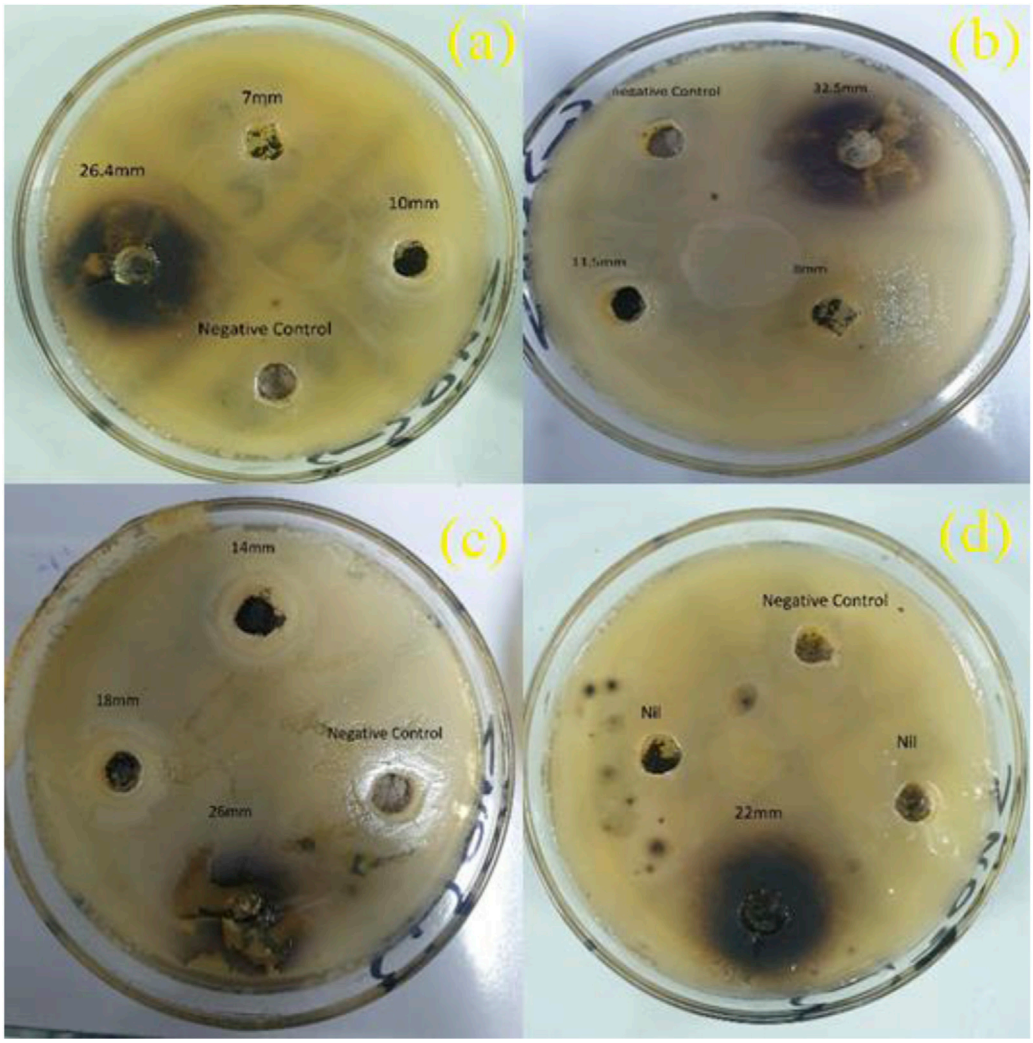

FIGURE 7
Zone inhibition to assess antibacterial activity **(A)** Activity of $Mn_2Se_3Cl_2O_7$ against *E. coli* **(B)** Activity of $Mn_2Se_3Cl_2O_7$ against *S. Aureus* **(C)** Activity of $SnSe_3O_4Cl$ against *E. coli* **(D)** Activity of $SnSe_3O_4Cl$ against *S. Aureus*.

TABLE 3 Antimicrobial activity of $Mn_2Se_3Cl_2O_7$ and $SnSe_3O_4Cl$.

Antibacterial activity					
Bacterial strains	Samples	Zone of inhibition (mm)			
		Blank	(0.25 mg/mL)	(0.5 mg/mL)	(1 mg/mL)
S. Aureus	$Mn_2Se_3Cl_2O_7$	0	8.0	11.0	32.5
	$SnSe_3O_4Cl$	0	14	18	26
E. Coli	$Mn_2Se_3Cl_2O_7$	0	7.0	10.0	26.4
	$SnSe_3O_4Cl$	0	Nil	Nil	22
Antifungal activity					
Fungal strains	Samples	Blank	(0.25 mg/mL)	(0.5 mg/mL)	(1 mg/mL)
Aspergillus flavus	$Mn_2Se_3Cl_2O_7$	0	9.0	12.0	33.9
	$SnSe_3O_4Cl$	0	13	20	29
Candida albicans	$Mn_2Se_3Cl_2O_7$	0	9.0	12.0	27.8
	$SnSe_3O_4Cl$	0	Nil	Nil	24

sample $Mn_2Se_3Cl_2O_7$ and $SnSe_3O_4Cl$ at low and high concentrations, statistically significant inhibition zones (mm) measuring 8–32.5 mm and 0–26.4 mm, respectively, were obtained. The maximum zone inhibition was observed for the Mn compound against *Staphylococcus aureus* and *Escherichia coli* (32.5 mm and 26.4 mm). On the other hand, the Mn compound significantly reduced the mycelial growth of *Aspergillus flavus* and *Candida albicans* (Table 3). The increase in the concentration of compounds shows a decrease in the concentration of bacterial colonies due to the formation of reactive oxygen species.

Particle size, shape, and surface-to-mass ratio of nanocomposites, which are crucial for antibacterial activity, are some of the variables that affect oxidative stress (Panáček et al., 2006; Ruparelia et al., 2008; Ruparelia et al., 2008; Hans et al., 2014). Reactive oxygen species (ROS) that damage bacterial membranes and promote the ejection of cytoplasmic contents and bacterial growth are produced effectively by nano-sized composites (Haider et al., 2019). This oxidative stress kills the bacterial DNA and inhibits the enzyme activity which is necessary for the growth of cells (Elkhoshkhany et al., 2017). The charge on the bacterial cell wall is negative while the overall charge on the metallic compound is positive (Tang and Lv, 2014). The cationic interaction of metal ions (Mn^{2+} and Sn^{4+}) with negatively charged bacterial cell walls is another possible mechanism for the death of bacteria (Aqeel et al., 2020). The bacterial and fungal cell wall layer consists of a network of covalently cross-linked peptide and glycan chains and is a proven target for antimicrobial agents that can provide great mechanical strength through osmotic lysis. There are two families of enzymes that play an important role in forming this layer, including transglycosylases and transpeptidases. At pH above 7, this peptide chain is negatively charged. These metal complexes can bind to peptide substrates in the peptidoglycan layer, preventing them from reacting with enzymes. However, the net effect is very similar, with reduced peptidoglycan cross-linking and consequent weakening of the cell wall (Schneider and Sahl, 2010; Ahmad et al., 2019; Wu et al., 2019).

Conclusion

In the present research, $Mn_2Se_3Cl_2O_7$ a dark brown crystalline material, and $SnSe_3O_4Cl$ have been synthesized by a solid-state reaction. The synthesized nanocomposite has been characterized by various spectroscopic techniques. After the successful formation of desired product, the composite has been tested to estimate the efficiency of the synthesized sample for dye degradation and antimicrobial activity. The presence of all the elements (Mn, Se, O, and Cl) was confirmed by the EDX spectrum. The result obtained by XRD proved that there must be a new phase present in it. The dye degradation efficiency was found to be 75% in the presence of $Mn_2Se_3Cl_2O_7$ having the rate constant value of 0.00447 $min^{-1.}$ Similarly, 71% of the dye is degraded in the presence of $SnSe_3O_4Cl$ having the rate constant value of 0.00378 $min^{-1.}$ The $Mn_2Se_3Cl_2O_7$ showed the maximum antimicrobial activity against Gram-positive bacteria i.e., 32.5 mm while 26.4 mm against Gram-negative bacteria. In the same way, the $SnSe_3O_4Cl$ showed the maximum antimicrobial activity against Gram-positive bacteria at 22 mm while 26 mm was against Gram-negative bacteria. These two newly synthesized compounds can be used as photo-catalysts and antimicrobial agents for the removal of organic pollutants from industrial effluents especially from the textile and food industry due to their proven efficiency against methylene blue dye and pathogens.

Data availability statement

The original contributions presented in the study are included in the article/supplementary material, further inquiries can be directed to the corresponding author.

Author contributions

All authors listed have made a substantial, direct, and intellectual contribution to the work and approved it for publication.

Acknowledgments

We are thankful to the Higher Education Commission of Pakistan for funding my research work under HEC funded project (No: 20-15745/NRPU/R&D/HEC/2021 2021). The authors express their appreciation to the Deanship of Scientific Research at King Khalid University, Saudi Arabia, for funding this work through research group program under grant number RGP. 2/167/43. This research was funded by Princess Nourah bint Abdulrahman University Researchers Supporting Project number (PNURSP2023R156), Princess Nourah bint Abdulrahman University, Riyadh, Saudi Arabia.

Conflict of interest

The authors declare that the research was conducted in the absence of any commercial or financial relationships that could be construed as a potential conflict of interest.

Publisher's note

All claims expressed in this article are solely those of the authors and do not necessarily represent those of their affiliated organizations, or those of the publisher, the editors and the reviewers. Any product that may be evaluated in this article, or claim that may be made by its manufacturer, is not guaranteed or endorsed by the publisher.

References

Ahmad, S., Wang, S., Wu, W., Yang, K., Zhang, Y., Tumukunde, E., et al. (2019). Functional analysis of peptidyl-prolyl cis-trans isomerase from Aspergillus. *flavus* 20, 2206. doi:10.3390/ijms20092206

Aliev, A., Kovrugin, V. M., Colmont, M., Terryn, C., Huvé, M., Siidra, O. I., et al. (2014). Revised bismuth chloroselenite system: Evidence of a noncentrosymmmetric structure with a giant unit cell. *Cryst. Growth Des.* 14, 3026. doi:10.1021/cg500293w

Alonso, J. A. (1998). Antimony (III) tellurium (IV) chloride trioxide $SbTeO_3Cl$: Synthesis and *ab initio* structure determination from X-ray and neutron powder diffraction data. *J. Chem. Soc. Dalton Trans.* (12), 1947–1950. doi:10.1039/A800799C

Altaf, S., Ajaz, H., Imran, M., Ul-Hamid, A., Naz, M., Aqeel, M., et al. (2020). Synthesis and characterization of binary selenides of transition metals to investigate its photocatalytic, antimicrobial and anticancer efcacy. *Appl. Nanosci.* 10, 2113–2127. doi:10.1007/s13204-020-01350-w

Altaf, S., Ijaz, H., Haider, J., Naz, M., Aqeel, M., Ul-Hamid, A., and Shahbaz, A. (2020). Influence of various transition metals incorporated into tellurium used as antimicrobial agent and textile dye degrader. *Appl. Nanosci.* 10 (11), 4241–4254. doi:10.1007/s13204-020-01547-z

Aqeel, M., Ikram, M., Asghar, A., Haider, A., Ul-Hamid, A., Naz, M., and Ali, S. (2020). Synthesis of capped Cr-doped ZnS nanoparticles with improved bactericidal and catalytic properties to treat polluted water. *Appl. Nanosci.* 10 (6), 2045–2055. doi:10.1007/s13204-020-01268-3

Bastide, B., Millet, P., Johnsson, M., and Galy, J. (2000). Synthesis of copper (II) and selenium (IV) oxochlorides by chemical transport reaction: Crystal structure of $Cu_9O_2(SeO_3)\ 4Cl_6$. *Mater. Res. Bull.* 35 (6), 847–855. doi:10.1016/S0025-5408(00)00279-8

Becker, R., Berger, H., and Johnsson, M. (2007). Monoclinic $Cu_3\ (SeO_3)\ 2Cl_2$: An oxohalide with an unusual CuO4Cl trigonal–bipyramidal coordination. *Acta Crystallogr. Sect. C. Cryst. Struct. Commun.* 63 (1), i4–i6. doi:10.1107/S0108270106050621

Becker, R., Johnsson, M., Kremer, R. K., Klauss, H. H., and Lemmens, P. (2006). Crystal structure and magnetic properties of $FeTe_2O_5X$ (X= Cl, Br): A frustrated spin cluster compound with a new Te (IV) coordination polyhedron. *J. Am. Chem. Soc.* 128 (48), 15469–15475. doi:10.1021/ja064738d

Becker, R., Prester, M., Berger, H., Lin, P. H., Johnsson, M., Drobac, D., et al. (2007). Crystal structure and magnetic properties of two new cobalt selenite halides: $Co_5\ (SeO_3)\ 4X2$ (X= Cl, Br). *J. Solid State Chem.* 180 (3), 1051–1059. doi:10.1016/j.jssc.2006.12.035

Berdonosov, P. S., Kuznetsova, E. S., and Dolgikh, V. A. (2018). Transition metal selenite halides: A fascinating family of magnetic compounds. *Crystals* 8, 159. doi:10.3390/cryst8040159

Bethi, B., Sonawane, S. H., Bhanvase, B. A., and Gumfekar, S. P. (2016). Nanomaterials-based advanced oxidation processes for wastewater treatment: A review. *Chem. Eng. Process. Process Intensif.* 109, 178–189. doi:10.1016/j.cep.2016.08.016

Castellote, M., and Bengtsson, N. (2011). "Principles of TiO_2 photocatalysis," in *Applications of Titanium Dioxide Photocatalysis to Construction Materials: State-of-the-Art Report of the RILEM Technical Committee 194-TDP*. Editors Y. Ohama and D. Van Gemert (Dordrecht, Netherlands: Springer), 5–10.

Charkin, D. O., Nazarchuk, E. V., Stefanovich, S. Y., Djangurazov, E. B., Zadoya, A. I., and Siidra, O. I. (2017). Polar $BaCl(ClO4) \cdot H2\ O$ layered chloride perchlorate. *Inorg. Chem. Commun.* 84, 174. doi:10.1016/j.inoche.2017.08.022

Chen, X., Yu, C., Guo, X., Bi, Q., Sajjad, M., Ren, Y., et al. (2018). *Cu2O nanoparticles/purity and used without any purification*. doi:10.1016/j.scitotenv.2018.01.078

Choudhury, A., Kumar, U., and Rao, C. N. R. (2002). Three-dimensional organically templated open-framework transition metal selenites. *Angew. Chem. Int. Ed.* 41, 158. doi:10.1002/1521-3773(20020104)41:1<158::aid-anie158>3.0.co;2-#

Elkhoshkhany, N., Reda, A., and Embaby, A. M. (2017). Preparation and study of optical, thermal, and antibacterial properties of vanadate–tellurite glass. *Ceram. Int.* 43 (17), 15635–15644. doi:10.1016/j.ceramint.2017.08.120

Farahmandjou, M., and Abaeiyan, N. (2017). Chemical synthesis of vanadium oxide (V2O5) nanoparticles prepared by sodium metavanadate. *J. Nanomed Res.* 5 (1), 00103. doi:10.15406/jnmr.2017.05.00103

Galy, J. (1979). *The crystal structure of a new oxide chloride of copper (II) and selenium Cu5Se2O8Cl2*. PASCAL8040060937.

Haider, A., Ijaz, M., Imran, M., Naz, M., Majeed, H., Khan, J., et al. (2019). Enhanced bactericidal action and dye degradation of spicy roots' extract-incorporated fne-tuned metal oxide nanoparticles. *Appl. Nanosci.* 1, 10. doi:10.1007/s13204-019-01188-x

Hans, M., Támara, J. C., Mathews, S., Bax, B., Hegetschweiler, A., Kautenburger, R., et al. (2014). Laser cladding of stainless steel with a copper–silver alloy to generate surfaces of high antimicrobial activity. *Appl. Surf. Sci.* 320, 195–199. doi:10.1016/j.apsusc.2014.09.069

Ijaz, H. (2007). *Contribution to the solid-state chemistry of chalcogeno halide of palladium, iron and indium*. Ph.D. Thesis (Germany: University of Siegen).

Jabeen, U., Shah, S. M., and Khan, S. U. (2017). Photo catalytic degradation of Alizarin red S using ZnS and cadmium doped ZnS nanoparticles under unfltered sunlight. *Surf. Interfac.* 6, 40–49. doi:10.1016/j.surfin.2016.11.002

Johnsson, M., Törnroos, K. W., Lemmens, P., and Millet, P. (2003). Crystal structure and magnetic properties of a new two-dimensional S = 1 quantum spin system Ni5(TeO3)4X2 (X = Cl, Br). *Chem. Mater.* 15, 68–73. doi:10.1021/cm0206587

Johnsson, M., Törnroos, K. W., Mila, F., and Millet, P. (2000). Tetrahedral clusters of copper (II): Crystal structures and magnetic properties of $Cu_2Te_2O_5X_2$ (X= Cl, Br). *Chem. Mater.* 12 (10), 2853–2857. doi:10.1021/cm000218k

Kannadasan, N., Shanmugam, N., Cholan, S., Sathishkumar, K., Viruthagiri, G., and Poonguzhali, R. (2014). The effect of Ce4+ incorporation on structural, morphological and photocatalytic characters of ZnO nanoparticles. *Mater. Charact.* 97, 37–46. doi:10.1016/j.matchar.2014.08.021

Kovrugin, V. M., Colmont, M., Mentré, O., Siidra, O. I., and Krivovichev, S. V. (2016). Dimers of oxocentred [OCu4] 6+ tetrahedra in two novel copper selenite chlorides, K [Cu3 O](SeO3) 2 Cl and Na2 [Cu7 O2] (SeO3) 4 Cl4, and related minerals and inorganic compounds. *Mineral. Mag.* 80, 227.

Kovrugin, V. M., Colmont, M., Siidra, O. I., Gurzhiy, V. V., Krivovichev, S. V., and Mentré, O. (2017). Pathways for synthesis of new selenium-containing oxo-compounds: Chemical vapor transport reactions, hydrothermal techniques and evaporation method. *J. Cryst. Growth* 457, 307. doi:10.1016/j.jcrysgro.2016.01.006

Kovrugin, V. M., Colmont, M., Siidra, O. I., Mentré, O., Al-Shuray, A., Gurzhiy, V. V., et al. (2015). Oxocentered Cu(ii) lead selenite honeycomb lattices hosting Cu(i)Cl2 groups obtained by chemical vapor transport reactions. *Chem. Commun.* 51, 9563. doi:10.1039/C5CC01426C

Kovrugin, V. M., Colmont, M., Terryn, C., Colis, S., Siidra, O. I., Krivovichev, S. V., et al. (2015). pH-controlled pathway and systematic hydrothermal phase diagram for elaboration of synthetic lead nickel selenites. *Inorg. Chem.* 54, 2425. doi:10.1021/ic503055v

Kovrugin, V. M., Krivovichev, S. V., Mentré, O., and Colmont, M. (2015). [NaCl] [Cu(HSeO3) 2], NaCl-intercalated Cu(HSeO3) 2: Synthesis, crystal structure and comparison with related compounds. *Z. Krist.* 230, 573. doi:10.1515/zkri-2015-1849

Krivovichev, S. V., Filatov, S. K., Armbruster, T., and Pankratova, O. Y. (2004)., 399. Kluwer Academic Publishers-Plenum Publishers, 226–228.Crystal structure of Cu (I) Cu (II) 4O (SeO3) Cl5, a new heterovalent $copp_er$ co_mpound, *Dokl. Chem.* doi:10.1023/B:DOCH.0000048084.41568.46

Krivovichev, S. V., Kahlenberg, V., Kaindl, R., Mersdorf, E., Tananaev, I. G., and Myasoedov, B. F. (2005). Nanoscale tubules in uranyl selenates. *Angew. Chem. Int. Ed. Engl.* 44, 1134. doi:10.1002/anie.200462356

Liu, B., Zhao, X., Terashima, C., Fujishima, A., and Nakata, K. (2014). Thermodynamic and kinetic analysis of heterogeneous photocatalysis for semiconductor systems. *Phys. Chem. Chem. Phys.* 16, 8751–8760. doi:10.1039/C3CP55317E

Lv, S.-W., Liu, J.-M., Zhao, N., Li, C.-Y., Wang, Z.-H., and Wang, S. (2020). A novel cobalt doped MOF-based photocatalyst with great applicability as an efcient mediator of peroxydisulfate activation for enhanced degradation of organic pollutants. *New J. Chem.* 44 doi:10.1039/C9NJ05503G

Millet, P., Bastide, B., and Johnsson, M. (2000). $Cu_3\ (SeO_3)\ 2Cl_2$: A new oxochloride of copper (II) and selenium (IV). *Solid state Commun.* 113 (12), 719–723. doi:10.1016/S0038-1098(99)00548-7

Millet, P., Johnsson, M., Pashchenko, V., Ksari, Y., Stepanov, A., and Mila, F. (2001). New copper (II)–lone electron pair elements–oxyhalides compounds: Syntheses, crystal structures, and magnetic properties. *Solid State Ionics* 141, 559–565. doi:10.1016/S0167-2738(01)00765-2

Mills, A., and Le Hunte, S. (1997). An overview of semiconductor photocatalysis. *J. Photochem. Photobiol. A Chem.* 108, 1–35. doi:10.1016/S1010-6030(97)00118-4

Ohtani, B. (2014). Revisiting the fundamental physical chemistry in heterogeneous photocatalysis: Its thermodynamics and kinetics. *Phys. Chem. Chem. Phys.* 16, 1788–1797. doi:10.1039/c3cp53653j

O'Shea, K. E., and Dionysiou, D. D. (2012). Advanced oxidation processes for water treatment. *J. Phys. Chem. Lett.* 3, 2112–2113. doi:10.1021/jz300929x

Ou, K., Wang, S., Wan, G., Huang, M., Zhang, Y., Bai, L., et al. (2017). A study of structural, morphological and optical properties of nanostructured ZnSe/ZnS multilayer thin flms. *J. Alloy Compd.* 726, 707–711. doi:10.1016/j.jallcom.2017.08.036

Panáček, A., Kvitek, L., Prucek, R., Kolář, M., Večeřová, R., Pizúrová, N., et al. (2006). Silver colloid nanoparticles: Synthesis, characterization, and their antibacterial activity. *J. Phys. Chem. B* 110, 16248–16253. doi:10.1021/jp063826h

Peng, W., Yang, C., and Yu, J. (2020). Bi2O3 and g-C3N4 quantum dot modifed anatase TiO2 heterojunction system for degradation of dyes under sunlight irradiation. *RSC Adv.* 10, 1181–1190. doi:10.1039/C9RA07424D

Photocatalysis, P. L. M. (2016). *Fundamentals and perspectives*. London, UK: The Royal Society of Chemistry, 1–28. CHAPTER 1 Photoelectrochemistry: From Basic Principles to Photocatalysis.

Pouretedal, H. R., Norozi, A., Keshavarz, M. H., and Semnani, A. (2009). Nanoparticles of zinc sulfide doped with manganese, nickel and copper as nanophotocatalyst in the degradation of organic dyes. *J. Hazard. Mater.* 162 (2-3), 674–681. doi:10.1016/j.jhazmat.2008.05.128

Rabbani, F., Shaikh, A. J., Khan, J., Ajaz, H., Rafique, M., Khan, Z. U. H., and Shah, G. M. (2019). Removal of organic colorants using nano copper antimony oxychloride synthesized by non-solvated system. *J. Inorg. Organomet. Polym. Mater.* 29 (3), 893–900. doi:10.1007/s10904-018-01063-2

Ranson, M., Cox, B., Keenan, C., and Teitelbaum, D. (2015). The impact of pollution prevention on toxic environmental releases from U.S. manufacturing facilities. *Environ. Sci. Technol.* 49, 12951–12957. doi:10.1021/acs.est.5b02367

Ruparelia, J. P., Chatterjee, A. K., Duttagupta, S. P., and Mukherji, S. (2008). Strain specifcity in antimicrobial activity of silver and copper nanoparticles. *Acta Biomater.* 4, 707–716. doi:10.1021/acs.est.5b02367

Schneider, J., Bahnemann, D., Ye, J., and Li, G. (2016). *Photocatalysis: Fundamentals and perspectives*. London, UK: Royal Society of Chemistry.

Schneider, T., and Sahl, H. G. (2010). An oldie but a goodie - cell wall biosynthesis as antibiotic target pathway. *Int. J. Med. Microbiol.* 300 (2–3), 161–169. doi:10.1016/j.ijmm.2009.10.005

Secuk, M. N., Aycibin, M., Erdinc, B., Gulebaglan, S. E., Dogan, E. K., and Akkus, H. (2014). *Ab-initio* calculations of structural, electronic, optical, dynamic and thermodynamic properties of HgTe and HgSe. *Am. J. Condens. Matter Phys.* 4 (1), 13–19. doi:10.5923/j.ajcmp.20140401.02

Semenova, T. F., Rozhdestvenskaya, I. V., Filatov, S. K., and Vergasova, L. P. (1992). Crystal structure and physical properties of sophiite, Zn_2 (SeO_3) Cl_2, a new mineral. *Mineral. Mag.* 56 (383), 241–245. doi:10.1180/minmag.1992.056.383.11

Shanmugam, N., Suthakaran, S., Kannadasan, N., and Sathishkumar, K. (2015). Synthesis and characterization of Te doped ZnO nanosheets for photocatalytic application. *JO Heterocycl.* 105, 15–20. doi:10.33805/2639-6734.105

Shanmugaratnam, S., and Rasalingam, S. (2019). "Transition metal chalcogenide (TMC) nanocomposites for environmental remediation application over extended solar irradiation," in *Nano catalyst* (London, United Kingdom: IntechOpen), 1–12.

Shen, Y. L., Mao, J. G., and Jiang, H. L. (2005). Synthesis, crystal structure and magnetic property of a new nickel selenite chloride: Ni5 (SeO_3) $4Cl_2$. *J. Solid State Chem.* 178 (9), 2942–2946. doi:10.1016/j.jssc.2005.07.005

Sivagowri, S., and Shivatharsiny, R. (2018). Transition metal chalcogenide (TMC) nanocomposites for environmental remediation application over extended solar irradiation. *In Nanocatalysts*, London, United Kingdom: IntechOpen.

Song, S. Y., Lee, D. W., and Ok, K. M. (2014). Rich structural chemistry in scandium selenium/tellurium oxides: Mixed-valent selenite– selenates, Sc2 (SeO3) 2 (SeO4) and Sc2 (TeO3)(SeO3)(SeO4), and ternary tellurite, Sc2 (TeO3) 3. *Inorg. Chem.* 53, 7040. doi:10.1021/ic501009c

Tang, Z. X., and Lv, B. F. (2014). MgO nanoparticles as antibacterial agent: Preparation and activity. *Braz. J. Chem. Eng.* 31, 591–601. doi:10.1590/0104-6632.20140313s00002813

Thermodynamic, W. (2012). Oxidation and reduction potentials of photocatalytic semiconductors in aqueous solution. *Chem. Mat.* 24, 3659–3666. doi:10.1021/cm302533s

von Gunten, U. (2018). Oxidation processes in water treatment: Are we on track? *Environ. Sci. Technol.* 52, 5062–5075. doi:10.1021/acs.est.8b00586

Wu, W. Z., Ahmad, S., Wang, S., Zhang, Y. F., Yang, H., Wang, S. H., et al. (2019). Expression and antibody preparation of small ubiquitin-like modifier (SUMO) from Aspergillus flavus. *IOP Conf. Ser. Earth Environ. Sci.* 346, 012002. doi:10.1088/1755-1315/346/1/012002

Ye, Z., Kong, L., Chen, F., Chen, Z., Lin, Y., and Liu, C. (2018). A comparative study of photocatalytic activity of ZnS photocatalyst for degradation of various dyes. *Optik* 164, 345–354. doi:10.1016/j.ijleo.2018.03.030

Zhang, D., Berger, H., Kremer, R. K., Wulferding, D., Lemmens, P., and Johnsson, M. (2010). Synthesis, crystal structure, and magnetic properties of the copper selenite chloride Cu_5 (SeO_3) 4Cl2. *Inorg. Chem.* 49 (20), 9683–9688. doi:10.1021/ic101431g

Zhang, D., Johnsson, M., Berger, H., Kremer, R. K., Wulferding, D., and Lemmens, P. (2009). Separation of the oxide and halide part in the oxohalide $Fe_3Te_3O_{10}Cl$ due to high Lewis acidity of the cations. *Inorg. Chem.* 48 (14), 6599–6603. doi:10.1021/ic9005778

Zhang, J., Jiang, F., and Zhang, L. (2004). Fabrication of single-crystalline semiconductor CdS nanobelts by vapor transport. *J. Phys. Chem. B* 108 (22), 7002–7005. doi:10.1021/jp036945v

Zhao, L.-D., He, J., Berardan, D., Lin, Y., Li, J.-F., Nan, C.-W., et al. (2014). BiCuSeO oxyselenides: New promising thermoelectric materials. *Energy Environ. Sci.* 7, 2900. doi:10.1039/C4EE00997E

Zhong, R., and DanruiNi, R. J. (2020). Cava Dicobalt (II) hydroxo-selenite: Hydrothermal synthesis, crystal structure and magnetic properties of Co_2SeO_3 $(OH)_2$. *J. Solid Stare Chem.* 285, 121250. doi:10.1016/j.jssc.2020.121250